

NJOY/JDKIM-01 26 November 199~~3~~2

**Testing of JENDL-3.1 and ENDF/B-VI based WIMS  
Cross-section Libraries Processed by NJOY91**

by

**Jung-Do Kim  
KAERI, Korea**

**Testing of JENDL-3.1 and ENDF/B-VI-based WIMS Cross Section  
Libraries Processed by NJOY91**

**Jung-Do Kim, Choong-Sub Gil and Hee-Kyung Kim**

**Korea Atomic Energy Research Institute  
P.O.Box 7, Daeduk-danji, Daejeon, 305-606, Korea**

*a draft presented at*

**1992 Symposium on Nuclear Data**

**November 26 ~ 27, 1992**

**JAERI, Tokai, Ibaraki-ken, Japan**

**Testing of JENDL-3.1 and ENDF/B-VI-based WIMS Cross Section Libraries**  
**Processed by NJOY91**

Jung-Do Kim, Choong-Sub Gil and Hee-Kyung Kim

Korea Atomic Energy Research Institute  
P.O.Box 7, Daeduk-danji, Daejeon, 305-606, Korea

The JENDL-3.1 and ENDF/B-VI-based 69-group cross section libraries for WIMS-D code were processed by using the latest version 91.38 of NJOY code system. The two multigroup libraries were intercompared by analyzing LWR critical experiments. By and large, the basic libraries show a similar tendency in the calculations of multiplication factor and integral lattice parameter.

### 1. Introduction

In the recent years, the new versions of evaluated nuclear data libraries have been released by Japan and USA. In order to test the quality and applicability of basic evaluated nuclear data libraries to light water reactors(LWR), 69-group constant libraries for WIMS code were generated by using the NJOY 91.38 nuclear data processing system with the JENDL-3.1<sup>1)</sup> and ENDF/B-VI<sup>2)</sup>, and an intercomparison work for the two multigroup libraries was performed by analyzing a number of LWR benchmark experiments recommended by the cross Section Evaluation Working Group(CSEWG)<sup>3)</sup>.

### 2. Processed Data

Processed nuclides in JENDL-3.1 and ENDF/B-VI for this work are the followings:

Nuclide	Identification Number	
	JENDL-3.1	ENDF/B-VI
1-H-1*	3011	125
8-O-16	3081	825
13-Al-27	3131	1325
92-U-235	3924	9228
92-U-238	3926	9237

\* Scattering Law Data (H in H<sub>2</sub>O) : ENDF/B-III

### 3. Data Processing

NJOY<sup>4)</sup> is well known as the most general purpose and versatile nuclear data processing code system, and the NJOY91.38 is the latest version released by the Los Alamos National Laboratory through the Radiation Shielding Information Center. The capabilities for processing ENDF-6 format file are almost complete.

To eliminate the differences due to the use of different processing method, input model, or definitions of multigroup constants as needed by the WIMS cross section library, two basic libraries were processed by using the NJOY91.38 with a same input option.

The specifications of multigroup processing used in the NJOY91.38 runs to provide WIMS library is given below and the processing scheme is shown in Figure 1.

☒ Reconstruction, linearization and thinning tolerance :	0.1%
☒ Temperature :	300°K
☒ Weighting function :	mid-life PWR flux (IWT=5 in GROUPE)
☒ Computed flux range :	0.1 eV ~ 48.052 eV for U-235 0.1 eV ~ 367.26 eV for U-238
☒ Dilution factor ( $\sigma_0$ ) :	$10^0, 10^1, 10^2, 10^3, 10^4, 10^5$ and $10^{10}$ barns for U-235 $10^{-1}, 10^0, 10^1, 5 \times 10^1, 10^2, 10^3$ and $10^{10}$ barns for U-238

### 4. Benchmark Problem

The CSEWG has recommended a variety of integral experiments for checking the data of interest for thermal reactor calculations. The experiments selected in this study include TRX and BAPL-UO<sub>2</sub> series with a simple geometric configuration.

The Westinghouse experiments known as the TRX lattices are frequently quoted as standards for benchmark calculations. The lattices were H<sub>2</sub>O-moderated, and fully reflected simple assemblies operated at room temperature. The fuel rods were of uranium metal clad in aluminum. Those of BAPL-UO<sub>2</sub> series were of high density uranium oxide. Brief characteristics of the lattices are summarized below.

Lattice	Fuel	Clad.	Fuel rad. (cm)	H <sub>2</sub> O/Fuel Volume Ratio
TRX-1	1.3% enriched	Al	0.4915	2.35
TRX-2				4.02
BAPL-1	1.3% enriched UO <sub>2</sub>	Al	0.4864	1.43
BAPL-2				1.78
BAPL-3				2.40

The following integral parameters were measured at the center of each lattices :

- Ratio of epithermal to thermal U-238 capture rate( $\rho^{28}$ ),
- ratio of epithermal to thermal U-235 fission rate( $\delta^{25}$ ),
- ratio of U-238 fission to U-235 fission rate( $\delta^{28}$ ) and
- ratio of U-238 capture to U-235 fission rate( $C^*$ ).

## 5. Calculation

WIMS code<sup>5)</sup> is one of the most widely used thermal reactor codes and is of interest especially to reactor physicists in developing countries. WIMS-KAERI (a KAERI version of WIMS-D4) calculations were performed using cylindrical cell model, 69 groups, discrete ordinates,  $S_{12}$ , and B-1 method for leakage. The calculated data are multiplication factors and integral lattice parameters.

## 6. Self-shielding of Elastic Scattering

In WIMS-type codes (CASMO or EPRI-CPM), self-shielding for absorption and fission reactions can be treated explicitly through resonance integral tabulations. However, resonance scattering cannot be taken into account in the same way. In order to consider the self-shielding effect of elastic scattering of U-238, another cross section set for U-238, which include fully self-shielded(dilution factor : 1.0 barn) scattering cross sections in the 69-group table(slowing-down power, transport cross section and scattering matrix), were generated.

## 7. Dilution Factor Grid

The dilution factor grid values should be chosen (by experience) to be concentrated in the  $\sigma_0$  range where the shielded cross section changes the most. To survey the sensitivity of calculated benchmark parameters to different dilution factor grid, another set with ten grids were processed with JENDL-3.1.

## 8. Results and Discussion

### 8.1 Effect of Dilution Factor Grid

Table 1 gives the influence of the grid. The 7 grids set gives a slightly higher  $K_{eff}$ , and lower  $\delta^{28}$  and  $C^*$  as compared with 10 grids set.

### 8.2 Multiplication Factor

Calculated eigenvalues are compared in Table 2. There are no significant differences in the  $K_{eff}$  values obtained with each of JENDL-3.1 and ENDF/B-VI, comparing with the large difference of computer running time for data processing (Table 3).

### 8.3 Integral Lattice Parameter

Intercomparison of reaction rate ratios, as well as calculated to experimental ratios (C/E), are summarized in Tables 4 ~ 7. The differences between JENDL-3.1 and ENDF/B-VI are about 1% or so.

### 8.4 Effect of Self-shielded Scattering

The calculated eigenvalues using the fully self-shielded U-238 scattering data are given in Table 8. The relative difference of  $k_{eff}$  values between no-shielded and fully-shielded scattering data are within 0.4 ~ 1.0%. In Table 9, the influence of U-238 self-shielded scattering on integral lattice parameters is summarized for JENDL-3.1. The relative changes in calculated parameters due to the self-shielded U-238 scattering are within 0.3 ~ 2.0%. Detailed results are given in Table 10.

### 8.5 Comparison of 69-group Data

69-group data processed with JENDL-3.1 and ENDF/B-VI are intercompared in Figures 2 ~12. Potential cross sections for O-16 and Al-27 give some differences. The ENDF/B-VI data of O-16 are about 3% larger and while those of Al-27 are approximately 5% smaller than the JENDL-3.1 data. Both libraries show a different shape for Al-27 absorption cross sections. Globally, U-235 capture cross sections of ENDF/B-VI show a lower tendency comparing with JENDL-3.1. Two libraries give -23 to 60% difference for U-235 capture cross sections and -19 to 44% difference for U-238 fission cross sections.

## 9. Conclusion

The JENDL-3.1 and ENDF/B-VI-based 69-group cross sections for WIMS library were processed by using the NJOY 91.38 system and the two libraries were intercompared by analyzing LWR critical experiments.

By and large, two libraries (JENDL-3.1 and ENDF/B-VI) show a similar tendency. The relative differences of  $k_{eff}$  and integral lattice parameters intercompared are within or not too far from the experimental uncertainty. The range of differences is within 0.2% on  $k_{eff}$  and around 1% on integral lattice parameters. The influence of self-shielded U-238 scattering on  $k_{eff}$  are within 0.4 ~ 1.0%. The  $k_{eff}$  values obtained with fully self-shielded U-238 scattering are underestimated.

## References

- 1) K. Shibada, et al. : JAERI-1319 (1990).
- 2) P. F. Rose : BNL-NCS-17541 4th ed. (1991).
- 3) "CSEWG Benchmark Specification", ENDF-202, BNL-19302 (1974).
- 4) R. E. MacFarlane, et al. : LA-9303-M, Vol. 1 (1982).
- 5) J. R. Askew, et al. : J. British Nuclear Energy Soc. 5, 564 (1966).

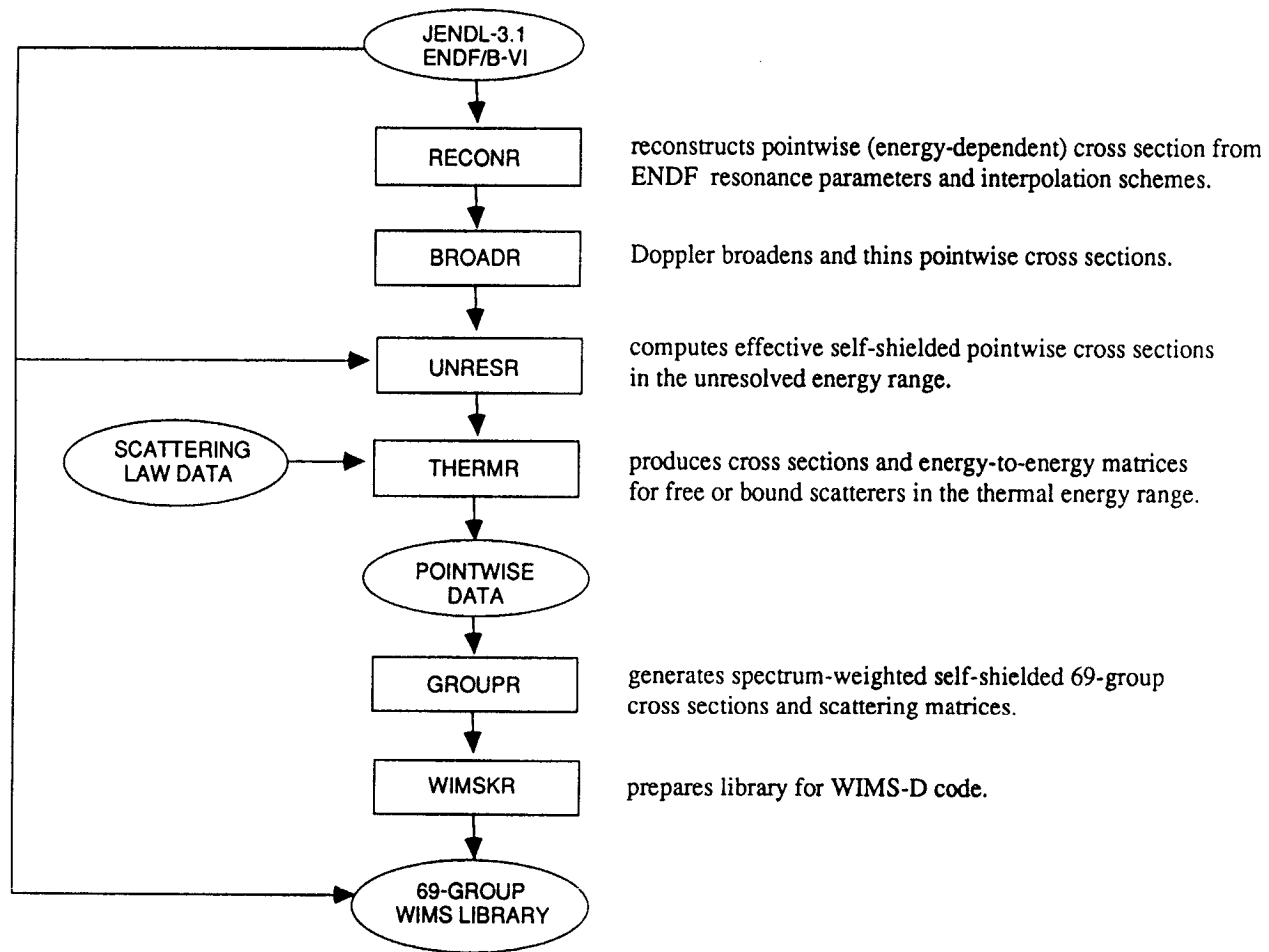


Figure. 1. Flow Diagram for Generating 69-group Library of WIMS-D Code

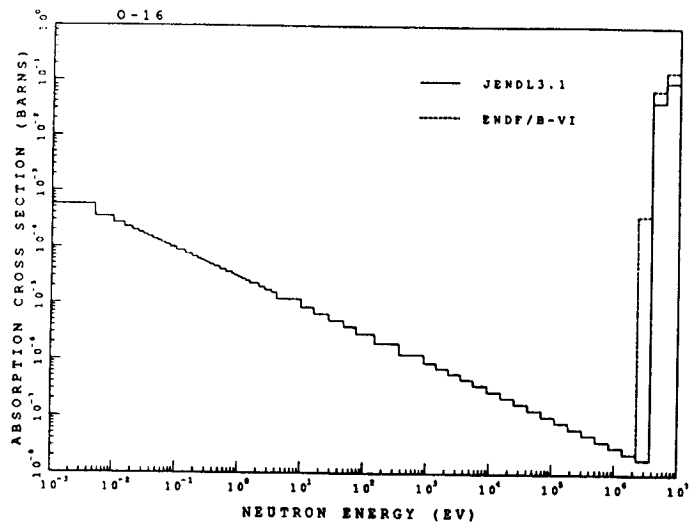


Fig. 2 Comparison of O-16 absorption cross sections.

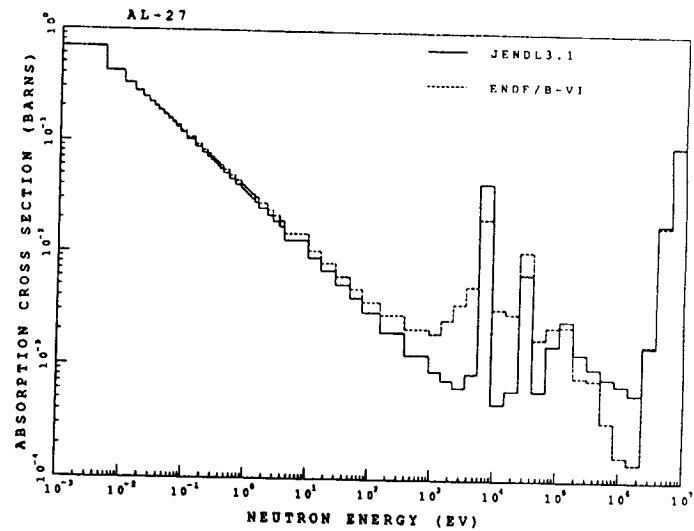


Fig. 4 Comparison of Al-27 absorption cross sections.

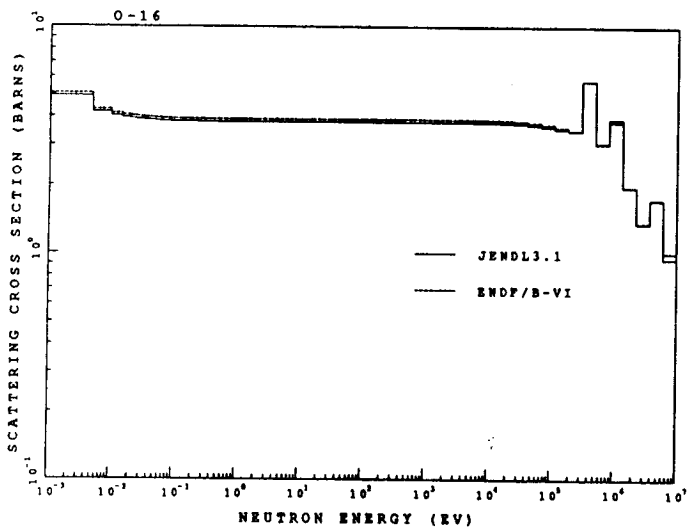


Fig. 3 Comparison of O-16 scattering cross sections.

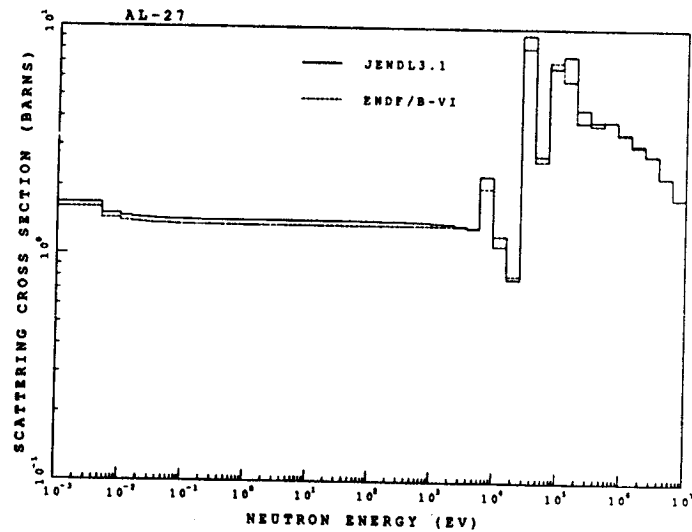


Fig. 5 Comparison of Al-27 scattering cross sections.

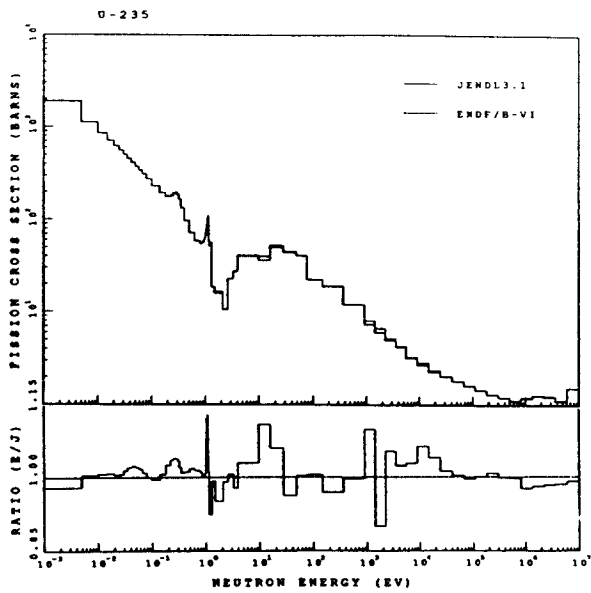


Fig. 6

Comparison of U-235 fission cross sections.

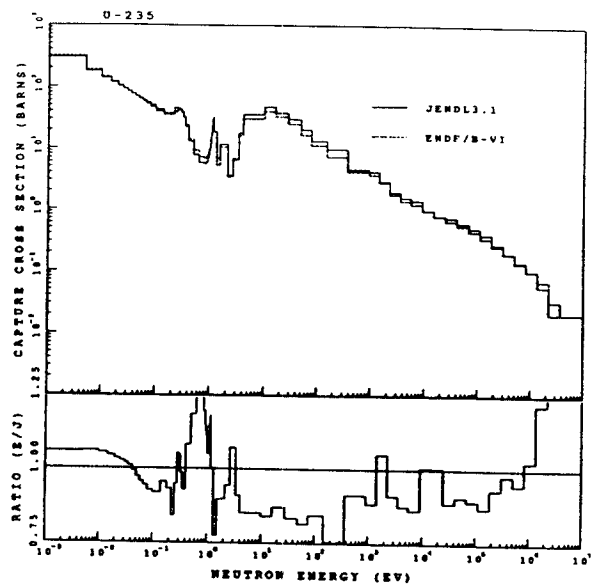


Fig. 7

Comparison of U-235 capture cross sections.

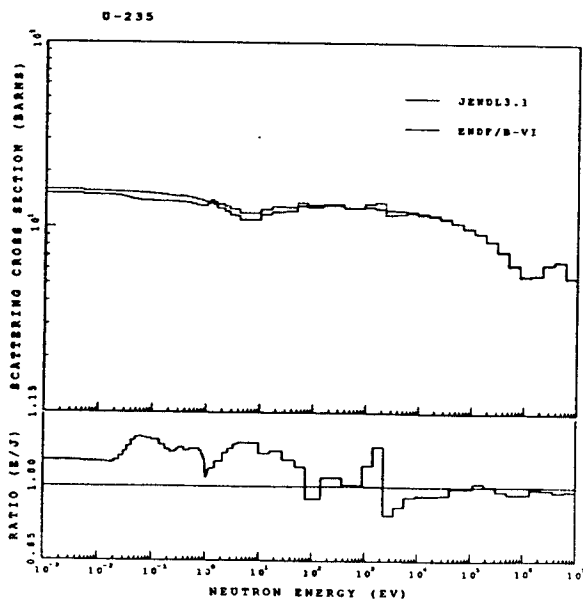


Fig. 8

Comparison of U-235 scattering cross sections.

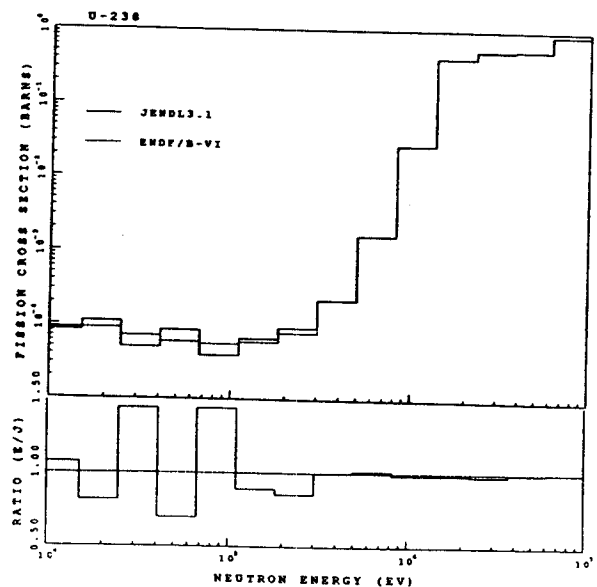


Fig. 9

Comparison of U-238 fission cross sections.

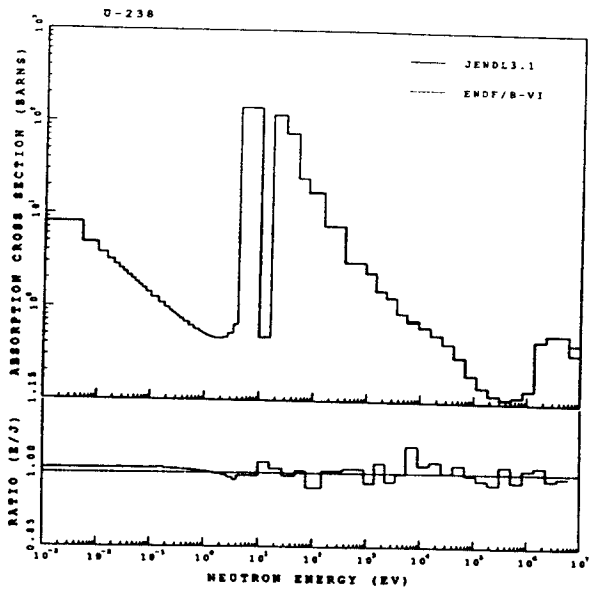


Fig. 10  
Comparison of U-238 absorption cross sections.

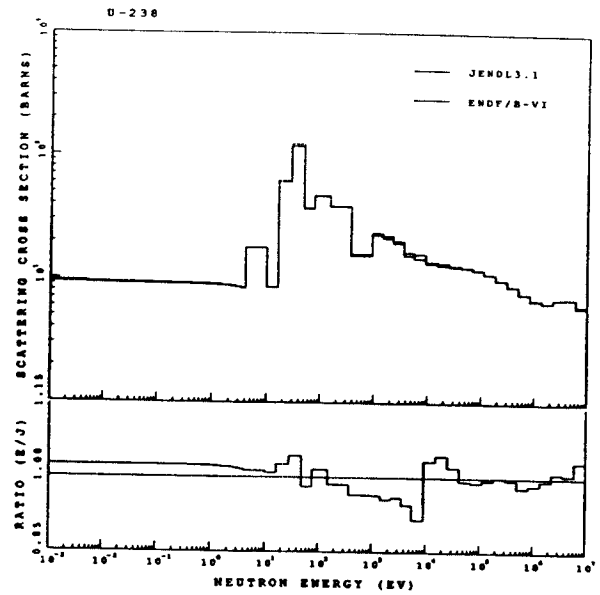


Fig. 11  
Comparison of u-238 scattering cross sections.

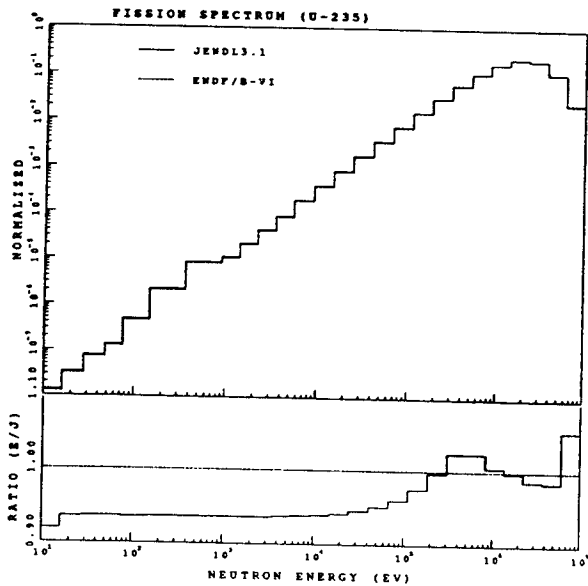


Fig. 12  
Comparison of U-235 fission spectrum.

Table 1. Effect due to Different Dilution Factor Grid

Lattice	No. of $\sigma_0$ grid		Percent difference
	7*	10**	
	K-effective		
TRX -1	0.9996	0.9988	+0.08
TRX -2	0.9979	0.9974	+0.05
BAPL-1	1.0035	1.0031	+0.04
BAPL-2	1.0025	1.0023	+0.02
BAPL-3	1.0015	1.0015	+0.00
	$\rho^{28}$		
TRX -1	1.3237	1.3292	-0.41
TRX -2	0.8322	0.8359	-0.44
BAPL-1	1.3903	1.3929	-0.19
BAPL-2	1.1591	1.1603	-0.10
BAPL-3	0.9128	0.9130	-0.02
	C*		
TRX -1	0.7881	0.7899	-0.23
TRX -2	0.6375	0.6388	-0.20
BAPL-1	0.8036	0.8044	-0.10
BAPL-2	0.7331	0.7335	-0.05
BAPL-3	0.6561	0.6562	-0.02

\* U-235 : 1, 10, 100,  $10^3$ ,  $10^4$ ,  $10^5$ ,  $10^{10}$   
 U-238 : 0.1, 1, 10, 50, 100,  $10^3$ ,  $10^{10}$

\*\* U-235 : 10, 50, 100, 150, 300, 500, 700,  $10^3$ ,  $10^4$ ,  $10^{10}$   
 U-238 : 0.1, 0.5, 1, 10, 30, 50, 70, 100,  $10^3$ ,  $10^{10}$

Table 2. Calculated Eigenvalues (using no-shielded scattering)

Lattice	K-infinite		K-effective	
	JENDL-3.1	ENDF/B-VI	JENDL-3.1	ENDF/B-VI
TRX -1	1.1782	1.1807 (+0.21)*	0.9996	1.0006 (+0.10)
TRX -2	1.1637	1.1646 (+0.08)	0.9979	0.9984 (+0.05)
BAPL-1	1.1416	1.1391 (-0.22)	1.0035	1.0012 (-0.23)
BAPL-2	1.1456	1.1432 (-0.21)	1.0025	1.0005 (-0.20)
BAPL-3	1.1319	1.1298 (-0.19)	1.0015	1.0000 (-0.15)

\* percent difference relative to JENDL-3.1

Table 3. Statistics of Uranium Data Processing

Content	Nuclide	Temperature	JENDL-3.1	ENDF/B-VI	Ratio
Number of X-section points processed with RECONR and BROADR routine	U-235	0°K	16,844 (16,114)*	381,820 (381,461)	22.7 (23.7)
		300°K	12,936	72,247	5.6
	U-238	0°K	325,542 (325,173)	551,910 (551,633)	1.7 (1.7)
		300°K	117,258	181,732	1.5
Computer running time(sec), Cyber 960-31 OS : NOS/VE	U-235	300°K	1,425	30,105	21.1
	U-238	300°K	24,908	83,130	3.3

\* Data in parenthesis are the number of resonance points

Table 4. Calculated and Calculated/Experimental(C/E) Values for Ratio of Epithermal to Thermal U-238 Capture Rate ( $\rho^{28}$ )

(using no-shielded scattering)

Lattice	JENDL-3.1		ENDF/B-VI	
	Calculated	C/E	Calculated	C/E
TRX -1	1.3237E+0	1.0028	1.3226E+0	1.0020 (-0.08)*
TRX -2	8.3221E-1	0.9943	8.3098E-1	0.9928 (-0.15)
BAPL-1	1.3903E+0	1.0002	1.4075E+0	1.0126 (+1.24)
BAPL-2	1.1591E+0	1.0349	1.1742E+0	1.0468 (+1.15)
BAPL-3	9.1285E-1	1.0076	9.2189E-1	1.0175 (+0.99)

\* percent difference relative to JENDL-3.1

Table 5. Calculated and Calculated/Experimental(C/E) Values for Ratio of Epithermal to Thermal U-235 Fission Rate ( $\delta^{25}$ ) (using no-shielded scattering)

Lattice	JENDL-3.1		ENDF/B-VI	
	Calculated	C/E	Calculated	C/E
TRX -1	9.4027E-2	0.9527	9.4549E-2	0.9579 (+0.56)*
TRX -2	5.7829E-2	0.9418	5.8149E-2	0.9471 (+0.56)
BAPL-1	7.9631E-2	0.9480	8.0229E-2	0.9551 (+0.75)
BAPL-2	6.5032E-2	0.9563	6.5511E-2	0.9634 (+0.74)
BAPL-3	5.0060E-2	0.9627	5.0419E-2	0.9696 (+0.72)

\* percent difference relative to JENDL-3.1

Table 6. Calculated and Calculated/Experimental(C/E) Values for Ratio of U-238 to U-235 Fission Rate ( $\delta^{28}$ ) (using no-shielded scattering)

Lattice	JENDL-3.1		ENDF/B-VI	
	Calculated	C/E	Calculated	C/E
TRX -1	9.6925E-2	1.0249	9.6099E-2	1.0169 (-0.78)*
TRX -2	6.9189E-2	0.9984	6.8430E-2	0.9874 (-1.10)
BAPL-1	7.5331E-2	0.9658	7.4574E-2	0.9561 (-1.00)
BAPL-2	6.4866E-2	0.9276	6.4120E-2	0.9160 (-1.15)
BAPL-3	5.3270E-2	0.9346	5.2564E-2	0.9222 (-1.33)

\* percent difference relative to JENDL-3.1

Table 7. Calculated and Calculated/Experimental(C/E) Values for Ratio of U-238 Capture to U-235 Fission Rate (C\*) (using no-shielded scattering)

Lattice	JENDL-3.1		ENDF/B-VI	
	Calculated	C/E	Calculated	C/E
TRX -1	7.8810E-1	0.9888	7.8708E-1	0.9876 (-0.13)*
TRX -2	6.3749E-1	0.9853	6.3687E-1	0.9843 (-0.10)
BAPL-1	8.0357E-1		8.0898E-1	(+0.67)
BAPL-2	7.3311E-1		7.3747E-1	(+0.59)
BAPL-3	6.5614E-1		6.5931E-1	(+0.48)

\* percent difference relative to JENDL-3.1

Table 8. Calculated Eigenvalues(using fully-shielded scattering)

Lattice	K-infinite		K-effective	
	JENDL-3.1	ENDF/B-VI	JENDL-3.1	ENDF/B-VI
TRX -1	1.1748	1.1772 (+0.20)*	0.9901	0.9908 (+0.07)
TRX -2	1.1616	1.1624 (+0.07)	0.9920	0.9924 (+0.04)
BAPL-1	1.1402	1.1376 (-0.23)	0.9975	0.9952 (-0.23)
BAPL-2	1.1445	1.1420 (-0.22)	0.9972	0.9951 (-0.21)
BAPL-3	1.1310	1.1288 (-0.19)	0.9976	0.9960 (-0.16)
percent difference relative to no-shielded scattering				
Lattice	K-infinite		K-effective	
	JENDL-3.1	ENDF/B-VI	JENDL-3.1	ENDF/B-VI
TRX -1	-0.29	-0.30	-0.95	-0.98
TRX -2	-0.18	-0.19	-0.59	-0.60
BAPL-1	-0.12	-0.13	-0.60	-0.60
BAPL-2	-0.10	-0.10	-0.53	-0.54
BAPL-3	-0.08	-0.09	-0.39	-0.40

\* percent difference relative to JENDL-3.1

Table 9. Influence of U-238 Self-shielded Scattering on Lattice Parameter (JENDL-3.1)

(percent difference relative to no-shielded scattering)

Lattice	$\rho^{28}$	$\delta^{25}$	$\delta^{28}$	C*
TRX -1	+1.98	+1.60	+1.07	+0.99
TRX -2	+1.79	+1.41	+0.64	+0.73
BAPL-1	+0.79	+0.63	+0.65	+0.41
BAPL-2	+0.77	+0.60	+0.57	+0.37
BAPL-3	+0.71	+0.56	+0.42	+0.31

Table 10. C/E Values for Integral Lattice Parameters

(using fully-shielded U-238 scattering)

Lattice	JENDL-3.1	ENDF/B-VI	JENDL-3.1	ENDF/B-VI
	$\rho^{28}$		$\delta^{25}$	
TRX -1	1.0227	1.0224	0.9679	0.9736
TRX -2	1.0120	1.0111	0.9552	0.9607
BAPL-1	1.0081	1.0209	0.9540	0.9613
BAPL-2	1.0428	1.0551	0.9621	0.9694
BAPL-3	1.0147	1.0251	0.9680	0.9751
	$\delta^{28}$		C*	
TRX -1	1.0358	1.0281	0.9986	0.9976
TRX -2	1.0048	0.9940	0.9925	0.9918
BAPL-1	0.9720	0.9624		
BAPL-2	0.9319	0.9213		
BAPL-3	0.9385	0.9261		